Collective effects in physisorbed molecular hydrogen on Ni/Au(111)

A. J. Therrien, A. Pronschinske, C. J. Murphy, E. A. Lewis, M. L. Liriano, M. D. Marcinkowski, and E. C. H. Sykes

Phys. Rev. B **92**, 161407 — Published 16 October 2015

DOI: 10.1103/PhysRevB.92.161407

Collective Effects in Physisorbed Molecular Hydrogen on Ni/Au(111)

A. J. Therrien, A. Pronschinske, C. J. Murphy, E. A. Lewis, M. L. Liriano, M. D. Marcinkowski, E. C. H. Sykes

Department of Chemistry, Tufts University, Medford, Massachusetts 02155-5813, USA

Abstract

We report a system in which the rotational, vibrational, electronic, and structural properties of condensed molecular H_2 can be measured with sub-nanometer precision using scanning tunneling microscopy. H_2 physisorbs around Ni nanoparticles on Au(111) and displays many non-classical characteristics, including unique disappearance upon heating that is due to changes in the time-averaged phonon ground state population. This collective phenomenon also gives rise to the appearance of sub-molecular features and constructive overlap at points where neighboring H_2 ensembles meet. A model based on the spatial distribution of collective excitations is proposed to explain these properties.

Main Text

Condensed molecular hydrogen offers a rich variety of physics including superfluid formation, phase transitions, electron transport, and nuclear-spin conversion, to name a few. The collective behavior of small clusters and films of H_2 at low temperature has long received considerable theoretical attention in terms of superfluid formation, [1-3] and it is expected that physisorbed H_2 forms gas and liquid-like phases on surfaces well below the bulk freezing point. Many experimental studies have focused on the behavior of hydrogen on surfaces at low temperature. [4-26] Some of the earliest work with physisorbed H_2 measured the rotational excitations by electron energy loss spectroscopy, which revealed that the molecule behaved as a quantum mechanical three-dimensional rigid rotor, despite the asymmetric interface environment. [4-6] It was also discovered that only para-H_2 and ortho-D_2 were present on the surface at low temperatures, as nuclear-spin flip relaxation is catalyzed on metal surfaces. [7,8]

Physisorbed H_2 has also been studied by inelastic electron tunneling spectroscopy (IETS) via scanning tunneling microscopy (STM) and nanojunctions. Understanding the mechanics of electron transport across a tunnel junction is crucial in designing molecular nanojunctions for applications in electronic devices. [9] This research indicated that H_2 molecules undergo two-state conformational switching. [11-21] The energy of this excitation is sensitive to H_2 coverage, STM tip state, and tip-surface separation. [17-21] Regardless of the *system-specific* excitation threshold for switching, one of the tunneling mechanisms was discovered to produce high-resolution spatial imaging while the other state yields conventional imaging. This technique is referred to as scanning tunneling hydrogen microscopy (STHM). In general, the apparent height of a feature imaged by STM is a convolution of topographic and electronic information, as STM is sensitive to the tip-surface separation, the local density of states, and the number of possible tunneling pathways. But the mechanics of the unique geometrical contrast of STHM is still not fully understood. [19]

Despite the previous IETS studies on physisorbed H_2, only very recently have rotational excitations been detected in such spectra. [21-23] Again, the molecule behaved as a three-dimensional rigid rotor, and measurements of H_2, HD, and D_2 rotation have been reported. Brune and co-workers used the model of Persson and Baratoff [27,28] to propose that rotational IETS features are enhanced via resonant tunneling. Therefore, the width and position of the molecular resonance state relative to the Fermi level of the surface may have led to the suppression of rotational features in other IETS studies. To control these parameters, Brune and co-workers grew an insulating layer of graphene or *h*-BN on Ni, Rh, or Ru to generate more appreciable conductance changes at the rotational threshold. [22] However, a decoupling layer was not required for Ho and co-workers to observe rotational excitations on Au(110), [21]

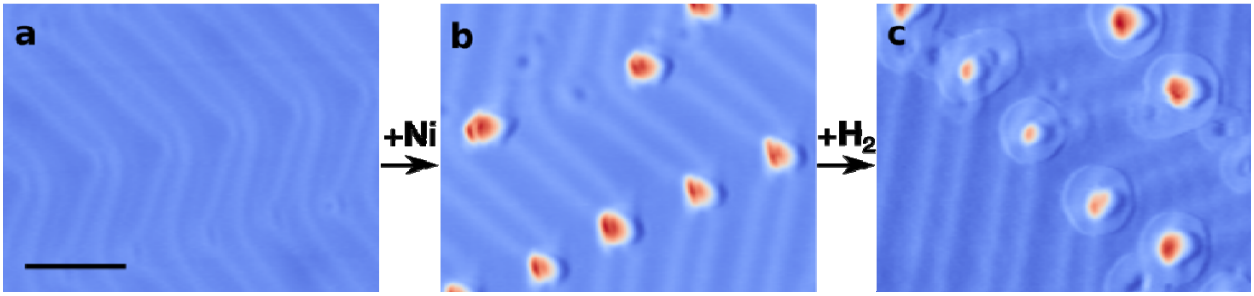

FIG. 1. 5 K STM images following the growth of Ni islands and physisorbed H_2 ensemble formation around Ni islands. (a) Image of the bare Au(111) 22 × √3 herringbone reconstruction (scale bar 10 nm), imaging conditions: 300 mV, 300 pA. (b) 0.04 ML Ni coverage on Au(111) deposited at a surface temperature of 430 ± 20 K. Ni islands preferentially nucleate at the elbows of the herringbone reconstruction while some Ni atoms substitute directly into the surface layer evidenced as depressions, imaging conditions: 300 mV, 300 pA. (c) Ni/Au(111) surface after 4 L exposure to H_2 at 5 K on which physisorbed H_2 ensembles form at Ni sites, imaging conditions: 30 mV, 30 pA.

although the signal was much weaker compared with H_2 on graphene or *h*-BN. [22,23] This was the first demonstration of H_2 rotational spectra on a bare metal surface by IETS, which raises the question of what makes Au(110) a more suitable substrate than Cu(111), [17,18] Ag(111), [19] or nanojunctions made of various metals. [9-16] It is also unclear if rotational IETS probes single molecules or molecular ensembles.

There is still much that is not understood about how H_2 molecules interact as a function of cluster size and temperature, and there are also questions about the mechanism by which STM images systems involving physisorbed H_2. In the present study we use Ni islands grown on Au(111) to nucleate physisorbed H_2 ensembles that display a range of unexpected properties. High-resolution STM imaging and IETS allows us to probe their spectral and temperature dependent properties and a quantum mechanical explanation for the observations is proposed. Imaging was conducted using an Omicron NanoTechnology 5 K STM. The Au(111) surface was prepared with Ar^+ sputtering and annealing to 1000 K. Ni deposition was performed in the preparation chamber using an electron beam evaporator with a deposition rate of ~0.04 ML min^{-1}. H_2 (Airgas, purity 99.999%) was then deposited onto the cooled surface. IETS curves were produced by numerical differentiation of I(V) curves with a Savitzky-Golay filter (2^{nd}-order polynomials fit to centered 14 mV windows). Color maps were applied to STM data using Gwyddion, [29] and edge shading was used to enhance the visibility of the molecular H_2 ensembles.

Figure 1 shows the growth of Ni islands on Au(111) at 430 ± 20 K and the subsequent nucleation of physisorbed H_2 ensembles at 5 K. For comparison, the bare Au(111) surface is shown in figure 1(a). The Ni/Au(111) alloy formation, shown in figure 1(b), agrees well with previous studies in which Ni atoms preferentially place exchange into the Au(111) surface at the elbows of the 22 × √3 herringbone reconstruction. [30] As the Ni coverage increases, islands one atomic layer high grow at these sites, [30-33] which consist of intermixed Ni and Au as evidenced by apparent height variations on the islands. [32] It is expected that the islands consist of a Ni-Au alloy due to the negative mixing enthalpy of the two metals. [34] Newly formed isolated depressions can also be seen on the terraces of Au(111) surface. These features are attributed to single Ni atoms substituted into the Au lattice, which appear as depressions due to the changes in electronic structure and the mismatch of surface lattice constants between Ni (2.49 Å) and Au (2.88 Å). [32] In Figure 1(c), in which the Ni/Au(111) surface alloy was exposed to H_2 at 5 K, physisorbed H_2 resides in well-defined ensembles at the Ni sites. It's clear that the ensembles consist of molecular H_2 and not H adatoms, which appear in STM images as depressions and have characteristic diffusion rates on the surface. [26] Physisorbed H_2 preferentially binds to the Ni islands due to an increase in van der Waals interactions with the ascending step edges and grow two-dimensionally, which is consistent with the growth of physisorbed H_2 in other studies. [18,20,23,24]

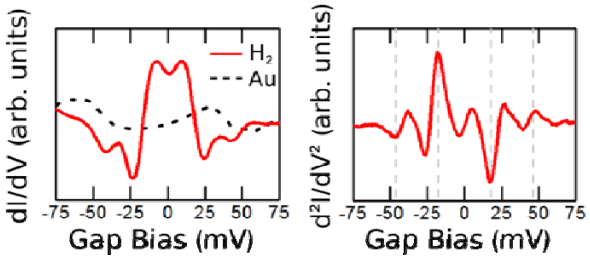

FIG. 2. First and second derivative curves of I(V) spectra. dI/dV spectra of both the H_2 ensembles and the neighboring Au(111) surface are shown. In the d^2I/dV^2 spectrum, transitions highlighted by the gray dotted grid lines are consistent with the conformational change of the molecule in the tunnel junction at the coverage studied (±17 meV) and J = 0 → 2 rotational excitation for H_2 (±45 meV). Curves are an average of 6 spectra taken at the same site.

Further evidence that the ensembles consist of molecular H_2 is found in the IETS spectra shown in figure 2. The dI/dV spectra of Au(111), the dotted black curve, is in agreement with previous literature, [35] indicating that H_2 is likely too mobile to measure on the Au surface away from Ni islands, or possibly does not reside there. Using the same STM tip as the spectra taken on Au(111) sites, measurements over H_2 ensembles reveal the J = 0 → 2 rotational excitation at ±45 meV, in good agreement with previous reports. [21-23] The IETS in figure 2 also shows that only para-H_2 is present on the surface, since no J = 1 → 3 excitation at ±73 meV for ortho-H_2 is detected. The other strong signals found at ±17 meV for H_2 in the IETS spectrum are due to conformational switching of the molecule in the tunnel junction. [11-21] As previously mentioned, the energy of the switching is extremely sensitive to coverage, tip state, and tip-surface separation. [17-21] There are also inelastic peaks around ±4 meV for H_2. These are phonon excitations of the ensemble, which is in agreement with the phonons identified by Brune and co-workers. [22,23] Similar low-energy signals are also present in the IETS of Ho and co-workers. [21]

After confirming that the ensembles consisted of molecular H_2, temperature-dependent STM imaging, in which the sample temperature is slowly raised (while correcting for thermal drift), allowed for examination of the evolution of the same set of H_2 ensembles. Figure 3 shows the real-time behavior of H_2 ensembles as the temperature was raised from 5 K to 11 K. Figure 3(b) clearly shows the apparent height reduction of the ensembles on top of and next to the Ni islands, which decreases at the same rate. The apparent height of the H_2 ensembles as a function of surface temperature is shown in figure 3(c). The height of the ensembles decreases to zero at 11 K. It is remarkable that during the heating ramp the H_2 ensembles occupy the same fixed area and do not change shape, but *decrease in apparent height*. The static boundary during heating is of particular interest because H_2 is known to desorb in UHV around 17 K, [8,24] and typically the diffusion barrier for an isolated molecule is approximately 12% that of the binding energy. [36] Most significantly, the slow and continuous decrease in apparent height is a clear deviation from classical solid two-dimensional layer desorption, which would begin from the edges inwards with the feature height remaining constant. [37]

Another non-classical observation involves the H_2 ensemble boundary, shown in figure 4. In figure 4(a), the internal lattice of the ensemble next to the Ni island is clearly resolved and is incommensurate with the underlying Au(111) surface. In figure 4(b) the same lattice is resolved both on top of and next to the Ni island, revealing hexagonal packing with a nearest-neighbor spacing of 0.40 ± 0.03 nm. This is in good agreement with two-dimensional H_2 packing on Cu(111) and the H_2 bulk spacing. [18] However, a major difference between H_2 on Cu(111) and H_2 on Ni/Au(111) can be seen at the boundary of the close-packed H_2. The edges of the ensembles in figure 4 are very well-defined and not kinked or facetted in a manner that would reflect the discreet nature of the H_2 molecules. Rather, the boundaries are smooth. In fact, at the interface of the Au(111) surface and the H_2 ensembles there appear to be incomplete units, or fractions of molecules. Similar effects appear with submonolayer coverages of H_2 on *h*-BN/Ni(111). [23,24] However, physisorbed H_2 on Cu(111) has been reported to be streaky, [18] indicative of molecular diffusion at time scales faster than STM measurements. Other studies of molecular layers, step atoms, and substituted surface atoms have shown that fractions of

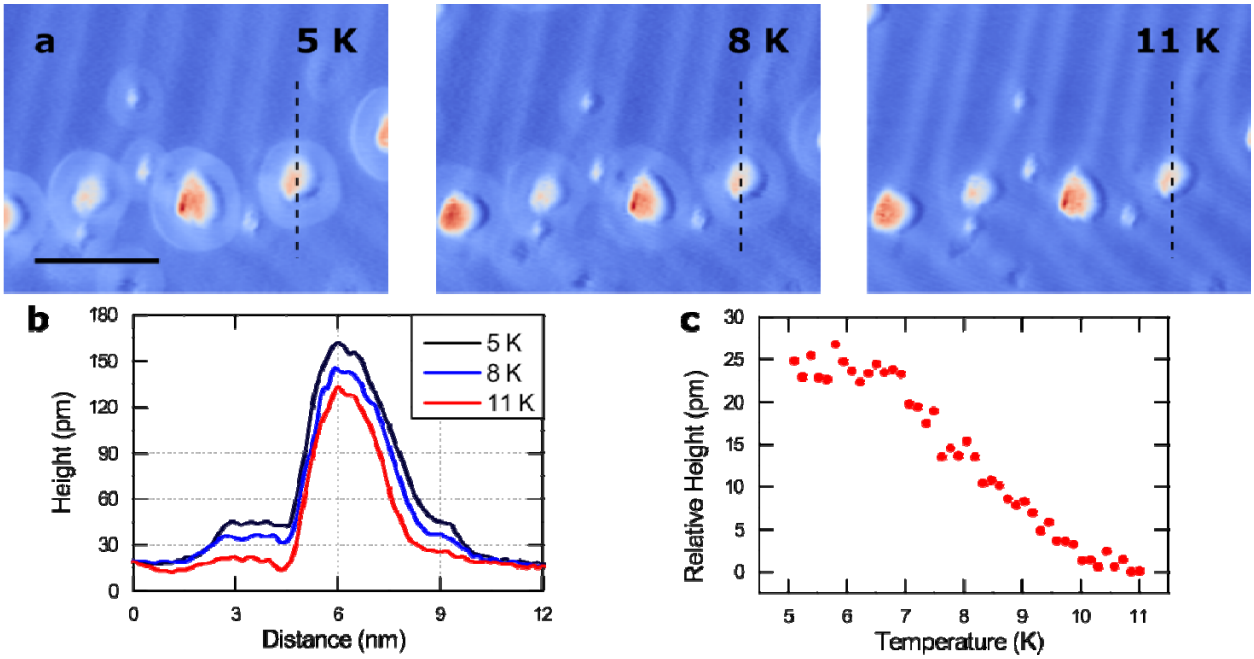

FIG. 3. (a) A series of STM images displaying the changes in the H_2 ensembles as the surface temperature increases from 5 K to 11 K (scale bar 10 nm). As the sample warms, the area that the ensembles occupy remains fixed and their shape is unchanged, however, the apparent height of the ensembles decreases leading to their disappearance around 11 K. See Supplemental Material at [URL] for the full series of STM images in the form of a time-lapse movie, imaging conditions: 40 mV, 40 pA. (b) Line scans at the position of the black dotted lines on each STM image plotted together. (c) The apparent height of a physisorbed H_2 ensemble relative to the Au(111) surface throughout the duration of the temperature ramp.

molecules can be observed if the molecules diffuse faster than the imaging rate. [26,38-41] These "partial molecule" features are dynamic and change from image to image, unlike the present data in which fractional molecules in the H_2 ensembles on Ni/Au(111) appear to be *static.* This can be explained by the spatial distribution of a quantized collective state available for tunneling, and not by the physical arrangement of molecules or time-averaged imaging of a dynamic system. This is further supported by the fact that the boundaries of the ensembles are static with respect to time and temperature.

Another unique characteristic of the molecular ensembles, shown in figure 4(c), is the manner in which two nearby H_2 ensembles overlap; rather than merge and form a continuous overlayer, there is an increase in the apparent height. This ensemble "overlap" is not consistent with bilayer growth for three reasons. First, the edges of the raised area are very smooth and not kinked, implying that it is not made up of discrete units. Second, the height at the intersection is less than double that of the adjacent ensembles. In figure 4(c), the height of the right-hand ensemble is 16 pm, the left-hand ensemble is 19 pm, and the overlap region is 26 pm. Third, bilayer growth would be expected to occur at the ensemble nucleation site, in this case the Ni islands, and not at the outer edges of the ensemble where the binding strength of molecules is weaker. Once again, this observation cannot be adequately described by classically interacting molecular islands.

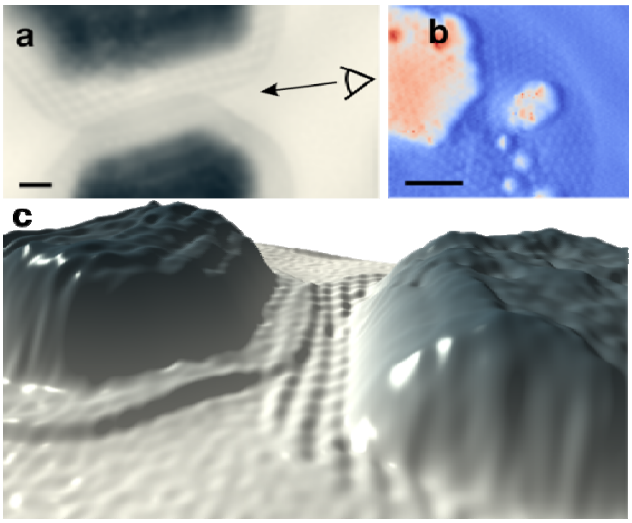

FIG. 4. (a) A high-resolution STM image of the "overlap" of two physisorbed D_2 ensembles (scale bar 1 nm), imaging conditions: 3 mV, 10 pA. (b) STM image of a H_2 ensemble boundary (scale bar 2 nm), imaging conditions: 200 mV, 10 pA. (c) Three-dimensional representation of (a) from the perspective of the arrow.

We propose that the present observations of H_2 ensembles can be explained by their quantum mechanical collective properties, namely phonon states. When the H_2 ensembles become large enough, low energy phonon states develop, which we and others have measured via IETS. [22,23] The Ni/Au(111) surface supports the growth of H_2 ensembles, whereas other (111) metal surfaces and nanojunctions do not, due to the high density of Ni step edges that can bind H_2 more strongly, coupled with sufficient surface area on the Au to accommodate a low-energy phonon state. The Au(110) 2 × 1 reconstructed surface also has a high step density and large surface area, which may explain the similarity in IETS features in this work with that on the Au(110). [21] As shown in figure 2, there is an available inelastic state on the H_2 ensembles, which is the low-energy phonon at ±4 meV, and is therefore present at all imaging biases. Inelastic excitation of the phonon state offers an additional tunneling pathway for electrons and results in an increase in conductance over the ensembles relative to Au. This can also be seen in the dI/dV spectra in figure 2; at ±4 mV the conductance of the H_2 ensembles is greater than Au(111) which is consistent with the fact that the ensembles appear higher than the bare Au(111) surface. This model also explains the H_2 ensemble "overlap," seen in figure 4(c). Two phonon states are present for electron tunneling at the ensemble intersection, offering increased conductance via both inelastic channels, resulting in increased apparent height where the two collective states meet. This model also sheds light on the static fractional molecules observed in figure 4, which can be explained by the spatial distribution of the phonon mode, rather than a conventional image of each molecule's position.

The phonon model also explains the disappearance of the H_2 ensembles in STM images at 11 K, shown in figure 3, even though H_2 doesn't desorb until about 17 K. This is due to a change in the phonon ground state population with temperature, not diffusion or evaporation of H_2. It has been shown that the substrate potential creates a gap in the phonon excitation spectrum, [23,25,42,43] resulting in a narrow energy range in which phonons can be excited. [23,25] As the sample temperature is raised, the ensembles spend an increased fraction of time in excited states. Thermal population of excited phonon states reduces the population of the ground phonon state, making the STM blind to the H_2 ensemble. On metals, phonon excitation and de-excitation occurs on time scales (< 1 ns) much faster than STM scanning (> 1 s). Therefore, the apparent height of an ensemble is a representation of the time-averaged ground state population of the phonon ground state. The measurement of the height of the ensembles is somewhat analogous to the zero-phonon band intensity of electronic transitions in Shpolskii matrices, in which the intensity of a spectral line is a function of the impurity-host coupling and population of thermally excited phonon modes. [44,45] The present system allows for the direct nanoscale spatial imaging of a collective state of a group of molecules.

In summary, we propose that a low-energy phonon mode present in physisorbed H_2 ensembles gives rise to the non-classical observations we report. The Ni/Au surface serves as a nanostructured nucleation array for H_2 clusters of controllable size exhibiting many quantum phenomena. It provides a system in which the range of collective molecular interactions can be

quantified by both structural imaging and spectroscopy with sub-nanometer precision. These findings are a step towards a full understanding the unique non-classical behavior of small H_2 clusters at low temperature.

Acknowledgements: The U.S. Department of Energy supported this work (Grant No. FG02-10ER16170). M.L.L. thanks the NSF for a Graduate Research Fellowship. E.C.H.S. thanks the Dreyfus Foundation for a Teacher-Scholar award and the Petroleum Research Fund for a New Directions grant.

References

[1] M. C. Gordillo and D. M. Ceperley, Phys. Rev. B 65, 174527 (2002).

[2] S. Idowu and M. Boninsegni, J. Chem. Phys. 140, 204310 (2014).

[3] T. Zeng and P.-N. Roy, Reports Prog. Phys. 77, 046601 (2014).

[4] P. Avouris, D. Schmeisser, and J. E. Demuth, Phys. Rev. Lett. 48, 199 (1982).

[5] S. Andersson and J. Harris, Phys. Rev. Lett. 48, 545 (1982).

[6] R. E. Palmer and R. F. Willis, Surf. Sci. 179, L1 (1987).

[7] T. Sugimoto and K. Fukutani, Phys. Rev. Lett. 112, 146101 (2014).

[8] K. Fukutani and T. Sugimoto, Prog. Surf. Sci. 88, 279 (2013).

[9] N. Agraït, A. L. Yeyati, and J. M. van Ruitenbeek, Phys. Rep. 377, 81 (2003).

[10] R. H. M. Smit, Y. Noat, C. Untiedt, N. D. Lang, M. C. van Hemert, and J. M. van Ruitenbeek, Nature 419, 906 (2002).

[11] A. Halbritter, P. Makk, S. Csonka, and G. Mihály, Phys. Rev. B 77, 075402 (2008).

[12] T. Nakazumi, S. Kaneko, and M. Kiguchi, J. Phys. Chem. C 118, 7489 (2014).

[13] W. Thijssen, D. Djukic, a. Otte, R. Bremmer, and J. van Ruitenbeek, Phys. Rev. Lett. 97, 226806 (2006).

[14] M. Trouwborst, E. Huisman, S. van der Molen, and B. van Wees, Phys. Rev. B 80, 081407 (2009).

[15] T. Nakazumi and M. Kiguchi, J. Phys. Chem. Lett. 1, 923 (2010).

[16] M. Kiguchi, K. Hashimoto, Y. Ono, T. Taketsugu, and K. Murakoshi, Phys. Rev. B 81, 195401 (2010).

[17] C. Lotze, M. Corso, K. J. Franke, F. von Oppen, and J. I. Pascual, Science 338, 779 (2012).

[18] J. Gupta, C. Lutz, A. Heinrich, and D. Eigler, Phys. Rev. B 71, 115416 (2005).

[19] R. Temirov, S. Soubatch, O. Neucheva, A. C. Lassise, and F. S. Tautz, New J. Phys. 10, 053012 (2008).

[20] K. Yang, W. Xiao, L. Liu, X. Fei, H. Chen, S. Du, and H. J. Gao, Nano Res. 7, 79 (2014).

[21] S. Li, A. Yu, F. Toledo, Z. Han, H. Wang, H. Y. He, R. Wu, and W. Ho, Phys. Rev. Lett. 111, 146102 (2013).

[22] F. D. Natterer, F. Patthey, and H. Brune, ACS Nano 8, 7099 (2014).

[23] F. D. Natterer, F. Patthey, and H. Brune, Phys. Rev. Lett. 111, 175303 (2013).

[24] F. D. Natterer, F. Patthey, and H. Brune, Surf. Sci. 615, 80 (2013).

[25] H. J. Lauter, V. L. P. Frank, P. Leiderer, and H. Wiechert, Phys. B Condens. Matter 156-157, 280 (1989).

[26] A. D. Jewell, G. Peng, M. F. G. Mattera, E. A. Lewis, C. J. Murphy, G. Kyriakou, M. Mavrikakis, and E. C. H. Sykes, ACS Nano 6, 10115 (2012).

[27] B. N. J. Persson and A. Baratoff, Phys. Rev. Lett. 59, 339 (1987).

[28] A. Baratoff and B. N. J. Persson, J. Vac. Sci. Technol. A Vacuum, Surfaces, Film. 6, 331 (1988).

[29] D. Nečas and P. Klapetek, Cent. Eur. J. Phys. 10, 181 (2012).

[30] J. A. Meyer, I. D. Baikie, E. Kopatzki, and R. J. Behm, Surf. Sci. 365, 647 (1996).

[31] A. G. Trant, T. E. Jones, J. Gustafson, T. C. Q. Noakes, P. Bailey, and C. J. Baddeley, Surf. Sci. 603, 571 (2009).

[32] W. G. Cullen and P. N. First, Surf. Sci. 420, 53 (1999).

[33] D. D. Chambliss, R. J. Wilson, and S. Chiang, Phys. Rev. Lett. 66, 1721 (1991).

[34] A. Christensen, A. V. Ruban, P. Stoltze, K. W. Jacobsen, H. L. Skriver, J. K. Nørskov, and F. Besenbacher, Phys. Rev. B 56, 5822 (1997).

[35] V. Madhavan, W. Chen, T. Jamneala, M. F. Crommie, and N. S. Wingreen, Science 280, 567 (1998).

[36] A. U. Nilekar, J. Greeley, and M. Mavrikakis, Angew. Chemie Int. Ed. 45, 7046 (2006).

[37] M. Lennartz, P. Broekmann, M. Arenz, C. Stuhlmann, and K. Wandelt, Surf. Sci. 442, 215 (1999).

[38] B. A. Mantooth, E. C. H. Sykes, P. Han, A. M. Moore, Z. J. Donhauser, V. H. Crespi, and P. S. Weiss, J. Phys. Chem. C 6167 (2007).

[39] T. Mitsui, M. K. Rose, E. Fomin, D. F. Ogletree, and M. Salmeron, Science 297, 1850 (2002).

[40] M. Giesen and G. S. Icking-Konert, Surf. Sci. 412-413, 645 (1998).

[41] H. Brune, J. Wintterlin, R. J. Behm, and G. Ertl, Phys. Rev. B 51, 13592 (1995).

[42] W. B. J. M. Janssen, T. H. M. van den Berg, and A. van der Avoird, Phys. Rev. B 43, 5329 (1991).

[43] A. D. Novaco, Phys. Rev. Lett. 60, 2058 (1988).

[44] É. V Shpol'skiĭ, Sov. Phys. Uspekhi 3, 372 (1960).

[45] F. P. Burke and G. J. Small, Chem. Phys. 5, 198 (1974)